

Synchronization effects in a dual-wavelength class-B laser with modulated losses

B. F. Kuntsevich¹ and A. N. Pisarchik^{2,*†}

¹*Stepanov Institute of Physics, National Academy of Sciences of Belarus, Avenue F. Skaryna, 68, 220072 Minsk, Belarus*

²*Centro de Investigaciones en Optica, A.C., Loma del Bosque, 115, Colonia Lomas del Campestre, 37150, Leon, Gto, Mexico*

(Received 20 October 2000; revised manuscript received 21 May 2001; published 26 September 2001)

Different types of synchronization: in-phase, antiphase, phase, and lag synchronization, as well as amplitude death have been found theoretically in a dual-wavelength class-B laser with modulated losses in one of the channels. Depending on the laser parameters, oscillations in master and slave channels can be either completely or partially synchronized. The conditions for the dual-wavelength regime have been established. The analysis has been performed on the basis of transfer functions of the master and slave channels.

DOI: 10.1103/PhysRevE.64.046221

PACS number(s): 05.45.Xt, 42.65.Sf, 42.55.Lt, 05.45.Pq

I. INTRODUCTION

During recent years, an interest in studying synchronization phenomena in various systems has increased significantly. The main reasons of such interest are the fundamental aspects of a deeper understanding of coherent dynamical behavior of coupled systems in different areas, including chemistry [1], physics, biology, and economics [2], as well as due to the important practical application to secure communications [3]. By *synchronization* is commonly meant that the states of ensembles of two and more coupled oscillators with different individual frequencies are properly adjusted.

It is known that depending on the coupling strength and individual frequencies of coupled systems, synchronization can be either *complete* so that the states of the interacting systems coincide (master-slave synchronization) or have opposite phases (antiphase synchronization) [4–6] or *partial* so that the states are slightly different [5]. Particular cases of partial synchronization are *phase synchronization*, when the phases of coupled oscillators are equal while their amplitudes are noncorrelated [7] and *lag synchronization*, when the amplitudes are correlated but one system lags in time behind the other [8]. In general, synchronization can be defined as the presence of a functional relation between the states of master and slave systems (*generalized synchronization* [9]). For stronger coupling or time delay in the coupling an intriguing effect arises where the oscillators pull each other off their limit cycles and collapse to a state of zero amplitude [10,11]. This effect known as *amplitude death* has been theoretically predicted by several authors [10,12,13] and recently demonstrated experimentally by Herrero *et al.* [14] with a pair of thermo-optical oscillators linearly coupled by heat transfer. However, to our knowledge, this effect has not been reported for laser systems.

Lasers are among the most convenient dynamical systems as for theoretical and experimental study of these phenomena for secure communications. The ability to synchronize coupled chaotic systems was first demonstrated by Pecora and Carroll in 1990 [6]. They have shown that two identical

chaotic systems can be made to synchronize by linking them with a common signal. Later, their method has been realized with two coupled Nd:YAG (yttrium aluminum garnet) lasers [15], two CO₂ lasers, one of which was driven by the output of another laser [16], and semiconductor lasers [17]. More recently, the synchronization effects have been demonstrated in a bidirectional Nd:YAG ring laser with modulated pumping [18], in arrays of three Nd:YAG lasers [19], in two Nd:YVO₄ microchip lasers [20], in two pulsing CO₂ lasers coupled through a common saturable absorber [21], in two erbium-doped fiber lasers [22], and in a microchip LiNdP₄O₁₂ laser array with self-mixing feedback modulation [23].

In this paper we study synchronization effects in a class-B laser with modulated losses in one of the coupled channels. The laser is formed by two-channel cavity with a common active medium that acted as a coupling. Such dual-wavelength optical sources have recently attracted much attention for potential applications in wavelength division multiplexes transmission systems and optical signal processing. In particular, a dual-wavelength CO₂ laser is promising in remote sounding of the atmosphere, isotope separation, and metrological applications [24,25]. In molecular gas lasers many wavelengths can be emitted as a result of several specified vibrational transitions. The dual-wavelength regime in a low-pressure cw CO₂ laser has been first realized in 1980 [26]. Some dynamical regimes of such a laser with fixed modulation depth and losses in both channels have been recently demonstrated experimentally [27]. The goal of the present study is a detailed theoretical analysis of synchronization phenomena in a dual-wavelength CO₂ laser in a wide range of modulation depths and frequencies, and further generalization of our approach to class-B lasers. We emphasize that such lasers with independent tuning in each channel is an optical analog of a system of two coupled oscillators. The coupling between lasing lines is realized through the rotational relaxation, i.e., collisional processes of gas molecules. In most of the previous works synchronization effects were studied versus the coupling strength. As distinct from the previous studies, all calculations in this work have been performed for the fixed coupling that is defined by the constant pressure and composition of the active medium. However, a change in the modulation frequency leads to a change in the time delay in the response of the

*Email address: apisarch@foton.cio.mx

†On leave from Stepanov Institute of Physics, National Academy of Sciences of Belarus, Minsk, Belarus.

population inversion in the slave channel to the loss modulation in the master channel. We demonstrate different stages of synchronization in the dual-wavelength laser: from complete synchronization to partial synchronization including phase and lag synchronizations. We report for the first time in laser systems on a combined (in-phase–antiphase) type of synchronization and an amplitude death effect when lasing in the master channel disappears and oscillations in the slave channel are damped out to reach a steady state. We also describe for the first time to our knowledge phase synchronization in coupled chaotic laser oscillators.

The paper is organized as follows. In Sec. II we describe the complete system of equations for a CO₂ laser, which accounts vibrational and rotational relaxation processes. In Sec. III we discuss the results of the simulations. The synchronization effects are generalized in Sec. IV to class-B lasers on the basis of a two-level model for the active medium conditions. Finally, the main conclusions are presented in Sec. V.

II. NUMERICAL MODEL

As a particular case of the class-B lasers [28], in which polarization effects can be adiabatically eliminated, we shall consider a system of equations successfully used earlier for the description of a single-wavelength CO₂ laser [29,30]. Below, in Sec. IV, the main results will be generalized to a simplest two-level model of the active medium.

For the sake of definiteness, we suppose a single-mode lasing in the centers of P20 and P16 lines within the 00⁰1-10⁰0 vibrational transition. Let the losses in the first channel (master) be modulated as follows: $k_1 = k_{10} + k_{11}[1 + \sin(2\pi\nu t)]$, where $2k_{11}$ and ν are the modulation amplitude (depth) and frequency and k_{10} is a constant loss. The losses in the second channel (slave) are fixed, $k_2 = k_{20}$. The same active medium is responsible for the lasing in both channels. Then the equations can be written as follows:

$$\frac{dM_1}{dt} = \beta_3 N_e M_0 + W_{NC} N_C (N_2 M_0 - N_0 M_1), \quad (1)$$

$$\begin{aligned} \frac{dN_1}{dt} = & \beta_1 N_e N_0 - W_{10} N_1 + W_{21} N_2 + B_1 u_1 (n_2^1 - n_1^1) \\ & + B_2 u_2 (n_2^2 - n_1^2), \end{aligned} \quad (2)$$

$$\begin{aligned} \frac{dN_2}{dt} = & \beta_2 N_e N_0 + W_{NC} N_N (N_0 M_1 - N_2 M_0) - W_{21} N_2 \\ & - B_1 u_1 (n_2^1 - n_1^1) - B_2 u_2 (n_2^2 - n_1^2), \end{aligned} \quad (3)$$

$$\frac{dn_1}{dt} = B_1 u_1 (n_2^1 - n_1^1) + B_2 u_2 (n_2^2 - n_1^2) - V_1 (n_1 - N_1), \quad (4)$$

$$\frac{dn_2}{dt} = -B_1 u_1 (n_2^1 - n_1^1) - B_2 u_2 (n_2^2 - n_1^2) - V_2 (n_2 - N_2), \quad (5)$$

$$\frac{dn_1^1}{dt} = B_1 u_1 (n_2^1 - n_1^1) - V_R (n_1^1 - F_1^1 n_1) - V_1 (n_1^1 - F_1^1 N_1), \quad (6)$$

$$\frac{dn_2^1}{dt} = -B_1 u_1 (n_2^1 - n_1^1) - V_R (n_2^1 - F_2^1 n_2) - V_2 (n_2^1 - F_2^1 N_2), \quad (7)$$

$$\frac{dn_1^2}{dt} = B_2 u_2 (n_2^2 - n_1^2) - V_R (n_1^2 - F_1^2 n_1) - V_1 (n_1^2 - F_1^2 N_1), \quad (8)$$

$$\frac{dn_2^2}{dt} = -B_2 u_2 (n_2^2 - n_1^2) - V_R (n_2^2 - F_2^2 n_2) - V_2 (n_2^2 - F_2^2 N_2), \quad (9)$$

$$\frac{du_1}{dt} = v \mu (\chi_1 y_1 - k_1) u_1, \quad (10)$$

$$\frac{du_2}{dt} = v \mu (\chi_2 y_2 - k_2) u_2, \quad (11)$$

where $y_1 = n_2^1 - n_1^1$ and $y_2 = n_2^2 - n_1^2$ are the rotational population inversions.

Here M_0 and M_1 are the relative populations of the fundamental and first excited vibrational levels of N₂; N_0, N_1 , and N_2 are the relative quasiequilibrium populations of the vibrational 00⁰0, 10⁰0, and 00⁰1 levels of CO₂; n_1 and n_2 are the relative quasi-nonequilibrium (instantaneous) populations of the vibrational 10⁰0 and 00⁰1 levels of CO₂; n_1^1, n_1^2 and n_2^1, n_2^2 are the relative populations of lower and upper laser rotational sublevels in the master and slave channels; N_e is the free-electron density in the active medium; W_{21} and W_{10} are the effective rates of the collisional relaxation in the 00⁰1-10⁰0 and 10⁰0-00⁰0 transitions; V_R is the rotational relaxation rate; V_1 and V_2 are the vibrational relaxation rates that describe the relaxation of the instantaneous populations n_1 and n_2 to their quasiequilibrium values N_1 and N_2 ; W_{NC} is the rate constant of the vibrational energy transfer from N₂ to CO₂; β_1, β_2 , and β_3 are the pumping rates of the vibrational levels of CO₂ and N₂ in the electric discharge; N_C and N_N are the volume densities of CO₂ and N₂; F_1^1, F_1^2 and F_2^1, F_2^2 are the normalized Boltzmann functions determining the portion of the molecules in the corresponding rotational sublevels in the master and slave channels; u_1, B_1 and u_2, B_2 are the radiation densities and spectral Einstein's coefficients for the master and slave channels; v is the speed of light in the active medium, and μ is the packing coefficient for the active medium in the cavity.

All necessary parameters were calculated on the basis of the analysis of the data presented in Refs. [25,31,32]. We assume that before the discharge switches on the active medium CO₂:N₂:He = 1:1:8 has a pressure of 15 Torr. When the discharge switches on, the dissociation reaches 50% [33]. The lengths of the active medium and cavity are taken to be 35 cm and 100 cm, respectively, and the temperature in the active medium is supposed to be 350 K. We assume in the

calculations that $M_0 = M_s - M_1$ and $N_0 = N_s - N_1 - N_2$, where M_s and N_s are the relative total populations of the corresponding states of the CO₂ and N₂ molecules at standard conditions in the absence of pumping and lasing.

III. RESULTS AND DISCUSSIONS

Numerical simulations on the basis of the complete model Eqs. (1)–(11) yield four stationary solutions. These solutions depend on the system parameters. The fixed point for two-level model of the active medium will be obtained analytically in Sec. IV A. Here we consider only the results for the case of a dual-wavelength lasing, which corresponds to periodic or chaotic oscillations in both channels. Such a dual-wavelength regime is the most interesting with a practical point of view.

A. Types of synchronization

The dual-wavelength CO₂ laser with modulated losses in one of the channels exhibits a wide range of dynamical regimes ranging from periodic to chaotic pulsations. Some dynamical regimes of this laser are illustrated in Fig. 1. The time evolution of the power densities at different modulation frequencies in the master and slave channels, u_1 and u_2 , are shown respectively on the left-hand and right-hand sides of the figure. The alternative component of the losses is shown for reference by the dashed lines. The analysis of the curves shown in Fig. 1 allows one to reveal the following synchronization regimes.

(i) At very low modulation frequency, *antiphase synchronization* is observed [Figs. 1(a) and 1(a')]. During one-half of the modulation period when the loss in the master channel is minimal [$\sin(2\pi\nu t) \leq 0$], the lasing exists only in the master channel, while in the slave channel it is absent. During the next half of the period when $\sin(2\pi\nu t) > 0$, the opposite situation is realized: the rectangular pulses lase in the slave channel while in the master channel the lasing is absent. These phases are repeated sequentially. Thus, in this case the quasistationary regimes are realized in both channels, i.e., the loss and gain coefficients have the same value: $\chi_i(t)y_i(t) = k_i(t)$ ($i = 1, 2$). Therefore, the pulses in the slave channel are flat [$k_2(t) = \text{const}$] and the pulses in the master channel lase in the opposite phase with the value of $k_1(t)$. In this regime the loss modulation leads to the switch between oscillations in the master and slave channels. By changing k_{11} it is possible to control the duration of the rectangular pulses in the master and slave channels: with increasing k_{11} the pulse duration in the master (slave) channel decreases (increases).

(ii) At higher modulation frequency, synchronization remains complete but the dynamics is more complex. Now the shape of the pulses is not rectangular and their duration becomes shorter. As seen from Figs. 1(b) and 1(b') the laser operates in the period-4 regime. In this case we observe mixed *in-phase–antiphase synchronization*. The phase of the large-amplitude pulses in the master channel coincides with the phase of the pulses in the slave channel so that in-phase dynamics is realized. However, the envelope of the pulses

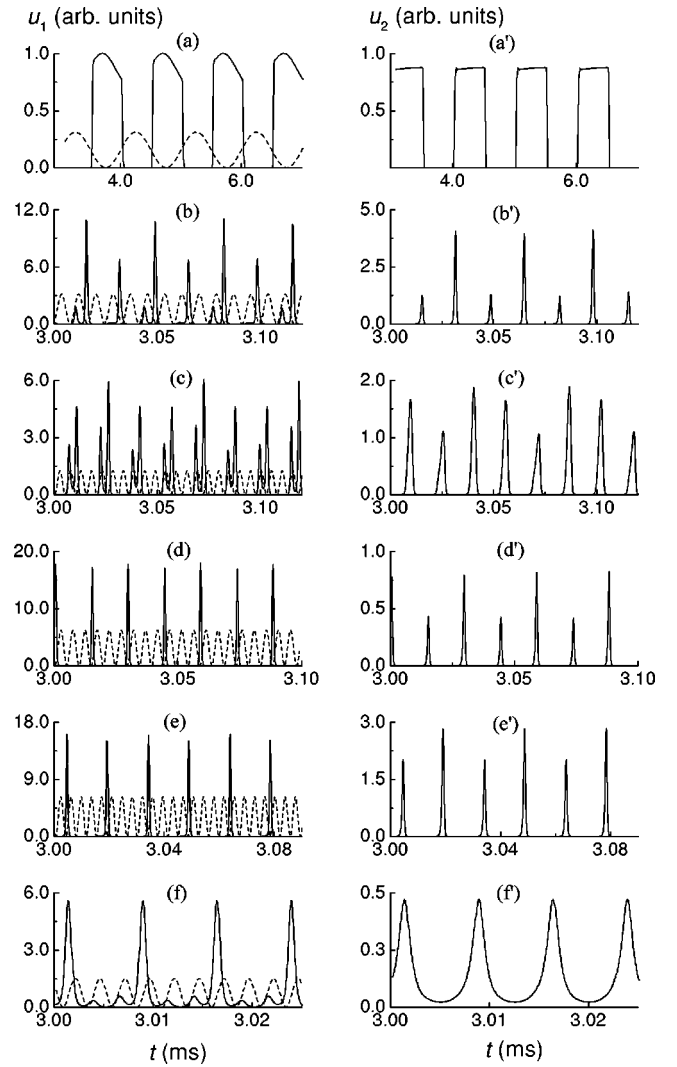


FIG. 1. Temporal behavior of radiation density of the dual-wavelength CO₂ laser in the master (left-hand column) and slave channels (right-hand column). The alternative losses are indicated by the dashed lines. $k_{10} = 3.11 \times 10^{-3} \text{ cm}^{-1}$, $k_{20} = 3.3 \times 10^{-3} \text{ cm}^{-1}$, $k_{11} = 3 \times 10^{-4} \text{ cm}^{-1}$. (a), (a') $\nu = 1$, (b), (b') 120, (c), (c') 195, (d), (d') 205, (e), (e') 270, and (f), (f') 400 kHz.

displays antiphase dynamics: the maximal (minimal) amplitudes in the master channels correspond to the minimal (maximal) amplitudes in the slave channel. In addition, we call attention to the double pulses in the master channel: the small-amplitude pulse comes before each large-amplitude pulse.

(iii) With further increase in the modulation frequency, synchronization becomes *partial*. In Figs. 1(c) and 1(c') *lag synchronization* is observed where both the pulses and their envelopes, even though they remain correlated, lag in time behind each other. The small-amplitude pulses also exist in the master channel and they are preceded by each large-amplitude pulse. The pulses in the slave channel lase between the small and large pulses in the master channel. As seen from these figures, the laser operates in the period-9 regime.

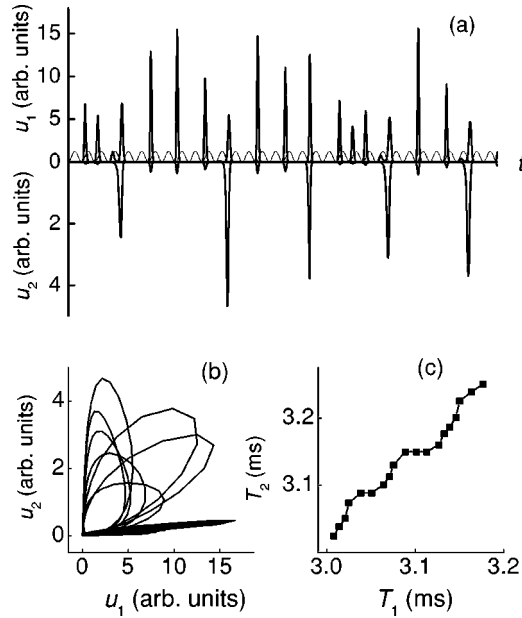


FIG. 2. (a) Phase synchronization of chaotic oscillations in the master and slave channels. The alternative losses are indicated by the thin line. (b) u_2 - u_1 plot shows that the amplitudes are noncorrelated. (c) Phase correlation. $k_{10}=3.1 \times 10^{-3} \text{ cm}^{-1}$, $k_{20}=3.3 \times 10^{-3} \text{ cm}^{-1}$, $k_{11}=3 \times 10^{-4} \text{ cm}^{-1}$, $\nu=160 \text{ kHz}$.

(iv) A small further increase in the modulation frequency makes the system again completely synchronized (*master-slave synchronization*) when the laser operates in the period-6 regime, as shown in Figs. 1(d) and 1(d'). The standard case of *complete synchronization* is also realized in the period-3 regime but with intermediate small peaks in the master channel [Figs. 1(f) and 1(f')].

(v) In Figs. 1(e) and 1(e') we demonstrate *in-phase-antiphase synchronization* as in Figs. 1(b) and 1(b') but the intermediate small pulses are absent. Here the laser operates in the period-8 regime.

(vi) Finally, *phase synchronization* of chaos is illustrated in Fig. 2. As seen from Fig. 2(a), the phases of the pulses in the master and slave channels are locked while the amplitudes remain noncorrelated and sustain an irregular motion of their own [see Fig. 2(b)]. In order to examine the phase correlation of the chaotic pulsations, the time of the n th peak for the slave channel, T_2 , is plotted against that for the master channel, T_1 , in Fig. 2(c).

B. Conditions for dual-wavelength regime and transfer functions

It is important, first, to establish conditions for the dual-wavelength regime because only in this regime synchronization can be possible. The conditions for realization of the dual-wavelength regime can be revealed from the analysis of transfer functions (TFs), i.e., amplitude-frequency characteristics of each channel. The TF describes the laser response to the parameter modulation. In Fig. 3 we plot the TFs of the master (left-hand column) and slave channels (right-hand column) for different k_{11} . Note, that the relation between k_{10} and k_{20} is chosen so that at $k_{11}=0$ the oscillations exist only

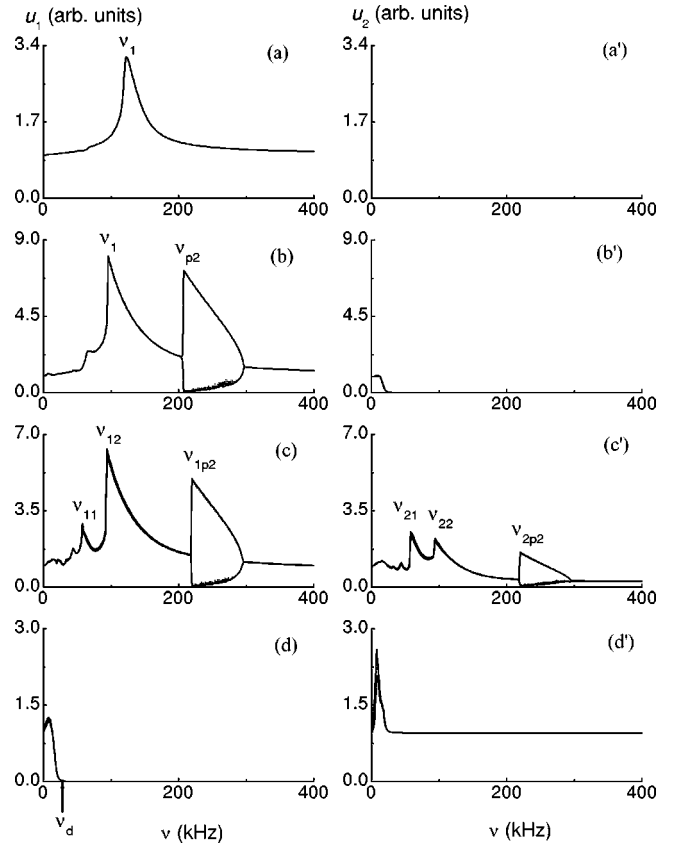


FIG. 3. Transfer functions of master (left-hand column) and slave channels (right-hand column) at different modulation amplitudes (a, a') $k_{11}=2 \times 10^{-5}$, (b, b') 8×10^{-5} , (c, c') 9.6×10^{-5} , and (d, d') $3 \times 10^{-4} \text{ cm}^{-1}$. $k_{10}=3.11 \times 10^{-3} \text{ cm}^{-1}$, $k_{20}=3.1 \times 10^{-3} \text{ cm}^{-1}$. Natural frequencies of the system are indicated in the figure.

in the master channel. In fact, the TFs shown in Fig. 3 are the bifurcation diagrams with the modulation frequency ν as a control parameter.

The general informative analysis of the results performed on the basis of the consideration of the TFs allows us to distinguish the following possible situations.

(i) At small k_{11} the conditions for the dual-wavelength regime is not reached and the laser operates in the single-wavelength regime [Figs. 3(a) and 3(a')]. The radiation emits only from the master channel whose TF has a standard shape of a *linear* response [29] with the single resonance (natural) frequency ν_1 .

(ii) With increasing k_{11} the laser response becomes *non-linear*. The maximum of the TF at ν_1 is shifted to the low-frequency region and a second resonance peak in the period-2 regime appears at the frequency $\nu_{p2} \approx 2\nu_1$ [Fig. 3(b)]. The necessary conditions for the appearance of oscillations in the slave channel is, first, a 100% modulation depth in the master channel. This condition can be achieved by increasing k_{11} . Second, no lasing time in the master channel should be sufficiently long for the development of oscillations in the slave channel. Here, the dual-wavelength regime is realized only in the low-frequency range, $\nu < 30 \text{ kHz}$ [Fig. 3(b')].

(iii) A further increase in k_{11} leads to the appearance of the *dual-wavelength* regime over all frequency range [Fig. 3(c) and 3(c')]. This results in three resonance frequencies in both channels, $\nu_{i1}=56$ kHz, $\nu_{i2}=98$ kHz, and $\nu_{ip2}=234$ kHz. The resonance frequencies of the laser can be presented as $\nu_{i1}=\nu_0-\Delta$ and $\nu_{i2}=\nu_0+\Delta$, where $\nu_0=(\nu_{i1}+\nu_{i2})/2$ is the average natural frequency and 2Δ is the mismatch between the resonance frequencies of the dual-wavelength laser. The resonance peaks in the period-2 regime appear at $\nu_{ip2}\approx 2\nu_0+2\Delta$.

When the slave channel is shut off and the laser operates in a single-wavelength regime, the energy is distributed only in the master channel. In this case the TF for the same laser parameters is quite different. It has only a single peak in the period-1 range that corresponds to the resonance frequency of the master oscillator $\nu_m=81$ kHz. The resonance frequency of the slave oscillator, $\nu_s=80$ kHz, was calculated when the master channel was shut off and the losses were modulated in the slave channel. One can see that these frequencies are very close to ν_0 and that the mismatch between these frequencies $\nu_m-\nu_s\ll 2\Delta$.

Note that systems of two coupled forced oscillators were investigated analytically in a linear approximation for mechanical and electric circuit systems [34]. A number of natural frequencies of such a coupled oscillatory system is equal to the number of its degrees of freedom. The dual-wavelength laser can be referred to as an optical analog of the coupled systems. In our case the laser has two degrees of freedom. The additional resonance peaks (at ν_{ip2}) appear due to nonlinear response of the system. The nonequality for the natural frequencies $\nu_{i1}<\nu_m, \nu_s<\nu_{i2}$ concurs with previous analysis [34].

The analysis shows that synchronization dynamics is governed by the relationship between the resonance frequencies and the modulation frequency. Antiphase synchronization is observed at $\nu<\nu_0$ and in-phase synchronization takes place at $\nu>\nu_0$. At the modulation near the average natural frequency of the system, $\nu\approx\nu_0$, when synchronization transforms from antiphase to in-phase, combined in-phase-antiphase and lag synchronization can be realized with double pulses in the master channel, as shown in Fig. 1(b) and 1(c).

(iv) Finally, in Figs. 3(d) and 3(d') we show the TFs for very high modulation amplitude ($k_{11}=3\times 10^{-4}$ cm⁻¹). In this case the lasing in the master channel occurs only at low frequencies, while in the slave channel the radiation exists over all frequency range. Due to the sluggishness of the system, the time intervals, at which the average loss coefficient in the master channel exceeds the average gain coefficient, increase. This leads to the disappearance of lasing in the master channel at $\nu=\nu_d$ and immediately results in the establishment of a steady state regime in the slave channel [horizontal line in Fig. 3(d')]. In fact, here we deal with a kind of *amplitude death*. This effect will be considered in Sec. III D in more details.

Thus, an increase in the modulation amplitude leads first to the enhancement of the laser response in the master channel and then to a decrease of oscillations and their disappearance. In the slave channel at the low-amplitude modulation

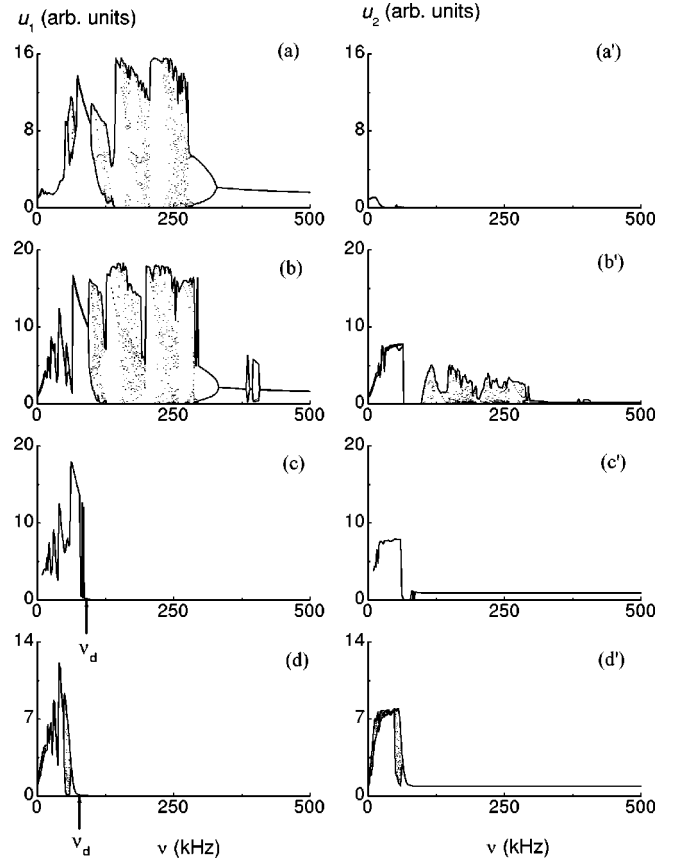


FIG. 4. Transfer functions of master (left-hand column) and slave channels (right-hand column) at laser modulation amplitudes (a, a') $k_{11}=2\times 10^{-4}$, (b, b') 3×10^{-4} , (c, c') 4×10^{-5} , and (d, d') 6×10^{-4} cm⁻¹. $k_{10}=3.11\times 10^{-3}$ cm⁻¹, $k_{20}=3.3\times 10^{-3}$ cm⁻¹.

the lasing is absent and with increasing amplitude the oscillations are developed. After that, the response in the slave channel decreases up to a steady state.

C. Large-amplitude modulation

We have already mentioned in Sec. III A about phase synchronization of chaos in the dual-wavelength laser. Now we shall consider the TFs of the laser with larger-amplitude modulation that can result in chaotic oscillations. Chaotic regimes can be realized when both the loss in the slave channel k_{20} and the modulation amplitude k_{11} are increased. In Fig. 4 we show the TFs for different k_{11} . At relatively small k_{11} the lasing in the master channel is observed over all frequency range [Fig. 4(a)], while in the slave channel the oscillations appear only at very low frequencies where the quasistationary regime is realized [Fig. 4(a')]. One can see that the TF of the master channel becomes more complex than in Fig. 3. It contains different periodic and chaotic ranges. Therefore it is not possible to distinguish the peaks of natural frequencies as in Sec. III B. With increasing k_{11} , the dual-wavelength regime is realized over wider frequency range [Figs. 4(b), 4(b'), and Figs. 4(c), 4(c')]. At very high k_{11} the oscillations in the master channel are suppressed and even disappear [Figs. 4(c) and 4(d)] and in the slave channel a steady state regime is reached [horizontal lines in Figs. 4(c') and 4(d')].

However, some features in synchronization can be distinguished for the large-amplitude case.

(i) At low modulation frequencies $\nu < 50$ kHz, for all cases *antiphase* synchronization takes place. At low modulation amplitude the dual-wavelength regime is observed only at low frequencies [Figs. 4(a) and 4(a')].

(ii) At $60 \text{ kHz} < \nu < 100 \text{ kHz}$ for the case shown in Figs. 4(b) and 4(b') *in-phase* synchronization is realized. The oscillations in the slave channel are suppressed to the very low level [the dip in Fig. 4(b')].

(iii) In the intermediate range $50 \text{ kHz} < \nu < 60 \text{ kHz}$ *negative lag* and *combined* synchronization take place.

(vi) At $\nu > 100$ kHz for the case shown in Figs. 4(b) and 4(b') the laser operates in the chaotic regime with *noncorrelated* oscillations.

(v) At high k_{11} the oscillations die at $\nu \geq \nu_d$ [Figs. 4(c) and 4(d)]. This case will be considered in the next section.

Thus, the type of synchronization can be changed with the modulation frequency and amplitude for various values of the constant cavity losses. The above calculations have been performed for the 00^01-10^00 lasing transition. However, additional investigation has shown that similar features hold also when the laser operates in other vibration-rotational transitions, for example, 00^01-02^00 , 00^02-10^01 , 00^02-02^01 , and 01^11-11^10 .

D. Amplitude death

Earlier theoretical studies showed that amplitude death occurs if the coupling between oscillators is sufficiently strong and when the natural frequencies are sufficiently disparate [12]. However, more recent investigations [13] indicate that the presence of time delay in the coupling removes this restriction. Time delay in the dual-wavelength laser appears due to finite relaxation times of the rotational sublevels of the CO_2 molecule and the delay in the rotation population inversion of the slave channel increases with the modulation amplitude.

The amplitude death for small and high cavity losses is seen in Figs. 3(d) and 4(c), 4(d). The oscillations in both channels disappear at large-amplitude modulation above the certain value of the modulation frequency through the Hopf bifurcation. In Fig. 5 we show the laser response when the slave channel is blocked (left-hand side) and when it is open (right-hand side) for the parameters corresponding to Fig. 3(d). Blocking the master channel, the large-amplitude oscillations are present in the master channel while they disappear after transients when both channels are open. The oscillations in the slave channel are damped out to reach a constant steady state while in the master channel the steady state is the noise level. The same situation is observed for the parameters corresponding to Fig. 4(d).

In Fig. 6 the death regions are shown at constant losses in the master and slave channels corresponding to Figs. 3 and 4 for different values of the modulation frequency. The death region ceases to exist below a certain threshold frequency ν_d . Below the death curves there exist different synchronization regimes exhibiting in-phase and antiphase oscillations or noncorrelated oscillations. As seen from Fig. 6 the onset

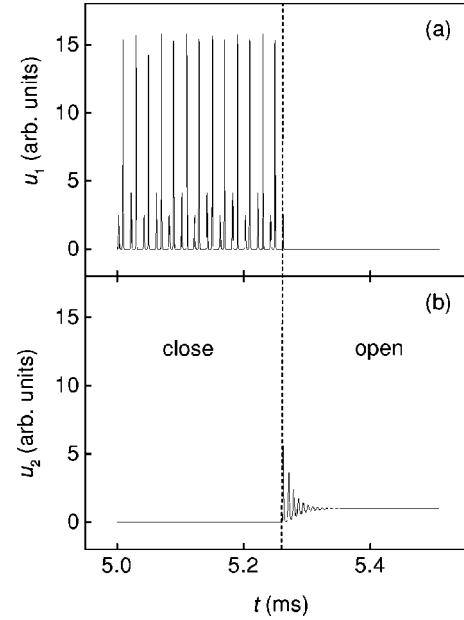


FIG. 5. Response of (a) master and (b) slave channels when the slave channel is blocked (left-hand side) and when it is open (right-hand side). The laser parameters are the same as for Fig. 3(d). $\nu = 100$ kHz.

frequency for the amplitude death ν_d and the modulation amplitude k_{11} are related by the following scaling law:

$$\nu_d \propto k_{11}^\alpha, \quad (12)$$

where the power $\alpha = -1/2$ is independent on the constant losses. A power law behavior at the transition between the death and phase locked regions has also been obtained by Ramana Reddy *et al.* [35] for limit cycle oscillators with a time delayed coupling.

E. Comparison with experiment

There are few works on experimental observation of the dual-wavelength radiation in lasers. However, some of our theoretical results can be compared with existing experimental results. For instance, the nonlinear TFs presented in Figs.

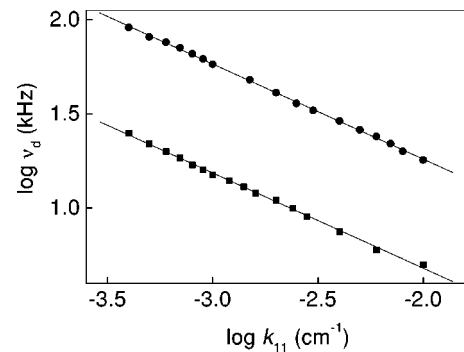


FIG. 6. Power law behavior of the death frequency vs the modulation amplitude for the parameters corresponding to Figs. 3 (squares) and 4 (dots). The slopes give the same scaling exponents $\alpha = -1/2$. The base of logarithms is 10.

3(c) and 3(c') are in a good agreement with experimental TFs presented in Ref. [27], where three resonance peaks were observed in the dual-wavelength CO₂ laser with modulated losses.

It is also of interest to compare our numerical results with the experimental ones obtained in other laser systems. Zenchenko *et al.* [36] studied experimentally the temporal behavior of a dual-beam Nd:YAG laser in which the coupling between two beams was realized by a partial overlap of the volumes in the active medium. The losses were modulated in one of the laser channels. They have observed antiphase synchronization at low-frequency modulation and in-phase synchronization at high-frequency modulation. There are also some other experimental works in different systems (see, for example, [34]), the results of which are in a good qualitative agreement with our results that confirms their validity and generality.

IV. TWO-LEVEL MODEL

The main results presented above can be generalized to the class-B lasers. The simplest two-level model of the active medium is used for this purpose (see, for example, [37]). The system of equations for the dual-wavelength laser can be written in the following form:

$$\frac{du_1}{dt} = v\mu(\kappa_1 y - k_1)u_1, \quad (13)$$

$$\frac{du_2}{dt} = v\mu(\kappa_2 y - k_2)u_2, \quad (14)$$

$$\frac{dy}{dt} = D[y_m - y(1 + R_1 u_1/D + R_2 u_2/D)], \quad (15)$$

where $\kappa_{1,2}$ and $R_{1,2}$ are the values proportional to the limiting gain coefficients and spectral Einstein's coefficients for the master and slave channels, y and y_m are the population inversion at the presence and absence of the field in the cavity, and D is the inversion relaxation rate.

The simplest system Eqs. (13)–(15) allows some analytical analysis for revealing the conditions of the dual-wavelength regime.

A. Equilibrium conditions and stability analysis

In order to simplify the analysis, we rewrite the system Eqs. (13)–(15) as follows:

$$\frac{du_1}{dt} = W_1(a_1 y - 1)u_1, \quad (16)$$

$$\frac{du_2}{dt} = W_2(a_2 y - 1)u_2, \quad (17)$$

$$\frac{dy}{dt} = D[y_m - y(1 + b_1 u_1 + b_2 u_2)], \quad (18)$$

where $W_i = v\mu k_i$ ($i = 1, 2$), $a_i = \kappa_i/k_i$, $b_i = R_i/D$, and we assume $k_i = k_{i0}$.

Setting $(du_1/dt) = (du_2/dt) = (dy/dt) = 0$ we obtain four equilibrium states for the system Eqs. (16)–(18).

(i) The first fixed point O_1 is trivial: $u_{10} = 0$, $u_{20} = 0$, and $y_0 = y_m$.

(ii) The second point O_2 corresponds to the absence of the lasing in the master channel: $u_{10} = 0$, $u_{20} = (a_2 y_m - 1)/b_2$ and $y_0 = 1/a_2$.

(iii) In the third point O_3 we find the opposite situation, the lasing is present in the master channel and absent in the slave channel: $u_{10} = (a_1 y_m - 1)/b_1$, $u_{20} = 0$, and $y_0 = 1/a_1$.

(iv) Finally, in point O_4 the lasing exists in both channels (*dual-wavelength regime*): $u_{10} \neq 0$ and $u_{20} \neq 0$. As follows from Eqs. (16) and (17), the last situation is possible only when $y_0 = 1/a_1 = 1/a_2 \equiv 1/a_0$. In this case $b_1 u_{10} + b_2 u_{20} = a_0 y_m - 1$. If $b_1 = b_2 = b_0$, then $u_{10} + u_{20} = (a_0 y_m - 1)/b_0$. This means that the sum of the radiation densities in the master and slave channels cannot exceed some critical number. The relationship between u_{10} and u_{20} in general case is defined by coefficients b_1 and b_2 . Note that for simplicity and by analogy with other works we assume that u_{10} and u_{20} are zero. Actually, these values cannot be less than some ‘‘noise’’ value of the radiation density.

Some qualitative information on the operation of the dual-wavelength laser for different system parameters can be obtained from stability analysis of the stationary solutions. A standard method of linearization of the initial system of equations near fixed points O_1 , O_2 , O_3 , and O_4 can be used for this purpose [34,38].

(i) If u_{10} , u_{20} , and y_0 are the coordinates of point O_1 , then the linearization of the equations in the vicinity of this point leads to the following characteristic equation:

$$\lambda^3 + c_1 \lambda^2 + c_2 \lambda + c_3 = 0, \quad (19)$$

where

$$c_1 = D - W_1(a_1 y_m - 1) - W_2(a_2 y_m - 1),$$

$$c_2 = W_1 W_2 (a_1 y_m - 1)(a_2 y_m - 1) - D[W_1(a_1 y_m - 1) + (W_2(a_2 y_m - 1))],$$

and

$$c_3 = W_1 W_2 D (a_1 y_m - 1)(a_2 y_m - 1).$$

If the real parts of all the eigenvalues λ_1 , λ_2 , and λ_3 are negative, then the equilibrium state is stable, i.e., it is an attractor (stable node or focus). If at least one of the roots of Eq. (19) has a positive real part, then the corresponding fixed point is unstable. Different signs of the roots indicate that the fixed point is a saddle point. If the eigenvalues are complex values, then the approach to the stationary regime has an

oscillatory character and the imaginary part of the eigenvalues defines the oscillation frequency.

The eigenvalues found from Eq. (19) are

$$\lambda_1 = W_1(a_1 y_m - 1), \quad \lambda_2 = W_2(a_2 y_m - 1), \quad \text{and} \\ \lambda_3 = -D. \quad (20)$$

Remember that point O_1 corresponds to the absence of lasing in both channels. Actually, it is evident from Eq. (20) that if the threshold conditions for lasing are fulfilled in none of the channels ($a_1 y_m < 1$ and $a_2 y_m < 1$), then point O_1 is an attractor, i.e., three eigenvalues are negative (stable node). If the threshold condition is fulfilled at least for one of the channels, then point O_1 becomes unstable, i.e., one of the eigenvalues is positive (saddle point).

(ii, iii) In a similar way one can find the eigenvalues for point O_2 ,

$$\lambda_{1,2} = -(a_2 y_m D/2) \pm [(a_2 y_m D/2)^2 - W_2 D(a_2 y_m - 1)]^{1/2}, \\ \lambda_3 = -W_1(1 - a_1/a_2), \quad (21)$$

and for point O_3 ,

$$\lambda_{1,2} = -(a_1 y_m D/2) \pm [(a_1 y_m D/2)^2 - W_1 D(a_1 y_m - 1)]^{1/2}, \\ \lambda_3 = -W_2(1 - a_2/a_1). \quad (22)$$

The equilibrium state O_j ($j=2,3$) can be realized when the lasing threshold is exceeded just in one of the channels while in the adjacent channel the threshold condition is not reached. In this case the following possible situations can be realized.

(1) Let us assume that a_j exceeds the corresponding value for the adjacent channel. Then for both fixed points $\lambda_3 < 0$. There can be two possibilities: (i) If $D(a_j y_m/2)^2 > W_j(a_j y_m - 1)$ (for instance, close to the lasing threshold), then $\lambda_{1,2} < 0$ and fixed point O_j is a stable node and (ii) if $D(a_j y_m/2)^2 < W_j(a_j y_m - 1)$, then $\lambda_{1,2}$ are complex and O_j is a stable focus.

(2) Let us suppose that a_j is less than the corresponding value for the adjacent channel. Then for both points $\lambda_3 > 0$. In this case (i) if $D(a_j y_m/2)^2 \geq W_j(a_j y_m - 1)$, then O_j is a saddle, and (ii) if $D(a_j y_m/2)^2 < W_j(a_j y_m - 1)$, then O_j is a saddle focus.

(iv) For point O_4 one of the eigenvalues always is equal to 0 (for example, $\lambda_1 = 0$) and two other eigenvalues are $\lambda_{2,3} = -(a_0 y_m D/2) \pm [(a_0 y_m D/2)^2 - W_0 D(a_0 y_m - 1)]^{1/2}$ while $W_1 = W_2 = W_0$. A zero eigenvalue is the characteristic property of the limit cycle. If in this case the threshold conditions in both channels are fulfilled and $D(a_0 y_m/2)^2 > W_0(a_0 y_m - 1)$, then λ_2 and λ_3 are also negative. This corresponds to a stable limit cycle, i.e., a periodic regime. In the next section the main attention will be just paid to a study of the most important regime of the periodic or chaotic oscillations in the dual-wavelength laser.

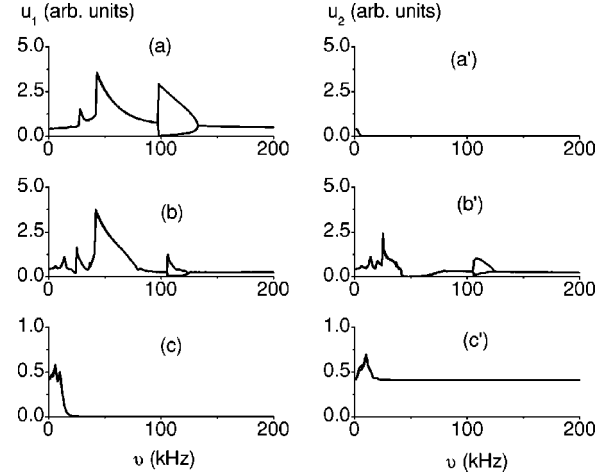


FIG. 7. Transfer functions of master (left-hand column) and slave channels (right-hand column) for two-level model at different modulation amplitudes (a, a') $k_{11} = 2.8 \times 10^{-5}$, (b, b') 4×10^{-5} , and (c, c') $5 \times 10^{-5} \text{ cm}^{-1}$. $k_{10} = 4 \times 10^{-3} \text{ cm}^{-1}$, $k_{20} = 3.9 \times 10^{-3} \text{ cm}^{-1}$.

B. Numerical results and discussion

The numerical simulation of the simplest model Eqs. (13)–(15) is performed in a similar way as in Sec. III. The same synchronization types have been observed at the following system parameters: $D = 1.4 \times 10^4 \text{ s}^{-1}$ and $y_m = 4.7 \times 10^{-2}$. For comparison we present in Fig. 7 the TFs for different modulation amplitudes. Similarly to the complete model (see Fig. 3) at small k_{11} the typical nonlinear response in the master channel with the resonance frequencies ν_1 and ν_{p2} is realized [Fig. 7(a)]. In the slave channel the lasing is observed only in the quasistationary range of the modulation frequencies [Fig. 7(a')]. The dual-wavelength regime can be reached at certain modulation amplitude [Figs. 7(b and b')]. As before, the peaks of the resonance frequencies $\nu_{11} = \nu_{21}$, where antiphase dynamics takes place, are presented. In the high-frequency range, the period-2 peaks are also observed ($\nu_{1p2} = \nu_{2p2}$). The absence of the resonance peak ν_{22} in the slave channel can be explained by (i) a strong competition between the laser channels due to ignoring rotational sublevels in the two-level model and (ii) the limitation condition $u_{10} + u_{20} = (a_0 y_m - 1)/b_0$ (see Sec. IV A). Antiphase and in-phase synchronizations are observed, respectively, at $\nu < \nu_0$ and $\nu > \nu_0$.

The amplitude death, as before, is observed at the relatively high modulation amplitude [Figs. 7(c and c')]. The same scaling law Eq. (12) has been obtained for the two-level model (Fig. 8), $\alpha = -0.53 \pm 0.03$. Thus, we have every reason to believe that this scaling law is universal and probably obeyed for different dynamical systems.

Finally, in Fig. 9 we illustrate phase synchronization of chaos for the two-level model.

Thus, it is seen from the short comparison that both models demonstrate the same qualitative relationship. Therefore, we believe that the synchronization effects considered in this paper can be observed in dual-wavelength lasers belonging to the class B as well as in other systems of two coupled oscillators with an external force in one of the channels.

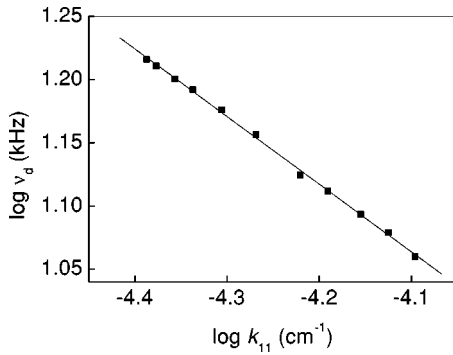


FIG. 8. Death frequency versus the modulation amplitude in log-log scale for the parameters corresponding to Figs. 7. The slope gives the scaling exponent $\alpha \approx -1/2$. The base of logarithms is 10.

V. CONCLUSIONS

In this paper we have studied theoretically synchronization phenomena in a dual-wavelength class-B laser with modulated losses in one of the channels. The detailed investigations have been performed on the basis of the complete laser model that describes well a real CO₂ laser with modulated parameters. The further analysis and numerical simulations made with the use of the two-level model of the active medium have shown that the main relationships are valid for the class-B lasers.

The conditions for the dual-wavelength lasing regime have been revealed. This regime can be realized when the excesses of the unsaturated gain over the losses in the master and slave channels are approximately equal. The analysis of transfer functions of the master and slave channels and their comparison allowed us to emerge general features in synchronization phenomena in the dual-wavelength class-B lasers. Several types of synchronization representing different degrees of correlation between the master and slave channels have been identified and are referred to as complete synchronization (in-phase, antiphase, and combined in-phase-antiphase synchronization), phase synchronization, and lag synchronization. The transfer functions of the dual-wavelength laser can contain resonance peaks corresponding to two natural frequencies of the system with two degrees of freedom and nonlinear (e.g., period-doubling) peaks. When the modulation frequency is closer to one of the natural frequencies, either antiphase or in-phase synchronization is realized. When the modulation frequency is between these frequencies, the intermediate combined type of synchronization takes place: the phases of the laser pulses and their envelopes are different. We have also demonstrated phase synchronization of chaotic oscillations.

We have observed for the first time in laser systems the amplitude death effect that appears at large modulation amplitudes. In this regime the lasing in the master channel disappears and the oscillations in the slave channel damp out to reach a steady state. This effect results from time delay in coupling due to finite relaxation rates in the active medium. We have found a particular scaling law with the power to be $-1/2$ in the transition between the death and oscillation re-

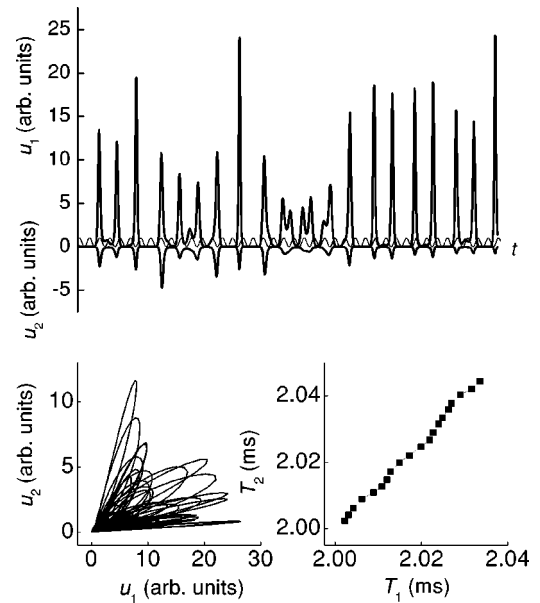


FIG. 9. (a) Phase synchronization of chaotic oscillations in the master and slave channels for the two-level model. The alternative losses are indicated by the thin line. (b) $u_2 - u_1$ plot shows that the amplitudes are noncorrelated. (c) Phase correlation. $k_{10} = 4 \times 10^{-3} \text{ cm}^{-1}$, $k_{20} = 3.9 \times 10^{-3} \text{ cm}^{-1}$, $k_{11} = 4.4 \times 10^{-5} \text{ cm}^{-1}$, $\nu = 92 \text{ kHz}$.

gions in the parameter space of the modulation amplitude and frequency. This scaling law is independent on the constant cavity losses. The same scaling law has been revealed with the use of the two-level model for the active medium. We believe that this scaling law is general and can be observed in other systems of coupled oscillators with external forcing in one of the channels.

It is important for some application to obtain a desirable shape of laser pulses, in particular, a rectangular shape. Some researchers (see, for example [39]) proposed to change the transmittance of the output mirror by a parabolic law. However, this is technically difficult to realize. Whereas the dual-wavelength regime allows one to obtain the rectangular pulses in the slave channel without any change in transmittance [see Fig. 1(a')].

Some results of our numerical calculations are in a good agreement with existing experimental data. We believe that different types of synchronization and amplitude death in a dual-wavelength laser that are related to different system parameters will be found in experiments and will have a number of applications, for example, for pulse shaping and in communications.

ACKNOWLEDGMENTS

This work has been supported in part by Consejo Nacional de Ciencia y Tecnología de México (CONACYT) (Project No. 33769-E), through a grant from the Institute Mexico-USA of the University of California (UC MEXUS) and CONACYT. B.F.K. acknowledges support from the Fundamental Research Fund of the Republic of Belarus.

- [1] Y. Kuramoto, *Chemical Oscillations, Waves and Turbulence* (Springer, Berlin, 1984).
- [2] E. Mosekilde, *Topics in Nonlinear Dynamics. Applications to Physics, Biology and Economics Systems* (World Scientific, Singapore, 1996).
- [3] M. Cuomo and A. V. Oppenheim, *Phys. Rev. Lett.* **71**, 65 (1993); L. Kocarev and T. Yamada, *Prog. Theor. Phys.* **69**, 32 (1983); L. G. Luo and P. L. Chu, *J. Opt. Soc. Am. B* **15**, 2524 (1998).
- [4] H. Fujisaka and T. Yamada, *Prog. Theor. Phys.* **69**, 32 (1983).
- [5] A. S. Pikovsky, *Z. Phys. B: Condens. Matter* **55**, 149 (1984).
- [6] L. M. Pecora and T. L. Carroll, *Phys. Rev. Lett.* **64**, 821 (1990).
- [7] M. G. Rosenblum, A. S. Pikovsky, and J. Kurths, *Phys. Rev. Lett.* **76**, 1804 (1996).
- [8] M. G. Rosenblum, A. S. Pikovsky, and J. Kurths, *Phys. Rev. Lett.* **78**, 4193 (1997).
- [9] N. F. Rulkov, A. S. Suschik, L. S. Tsimring, and H. D. I. Abarbanel, *Phys. Rev. E* **51**, 980 (1995).
- [10] K. Bar-Eli, *Physica D* **14D**, 242 (1985).
- [11] M. Crowley and I. Epstein, *J. Phys. Chem.* **93**, 2496 (1989).
- [12] D. G. Aronson, G. B. Ermentrout, and N. Kopell, *Physica D* **41**, 403 (1990); G. B. Ermentrout, *ibid.* **41D**, 219 (1990); P. C. Matthews and S. H. Strogatz, *Phys. Rev. Lett.* **65**, 1701 (1990); R. E. Mirollo and S. H. Strogatz, *J. Stat. Phys.* **60**, 245 (1990).
- [13] D. V. Ramana Reddy, A. Sen, and G. L. Johnston, *Phys. Rev. Lett.* **80**, 5109 (1998).
- [14] R. Herrero, M. Figueras, J. Rius, F. Pi, and G. Orriols, *Phys. Rev. Lett.* **84**, 5312 (2000).
- [15] R. Roy and K. S. Thornburg, Jr., *Phys. Rev. Lett.* **72**, 2009 (1994).
- [16] T. Sugawara, M. Tachikawa, T. Tsukamoto, T. Shimizu, *Phys. Rev. Lett.* **72**, 3502 (1994).
- [17] C. R. Mirasso, P. Colet, and P. G. Fernandez, *IEEE Photonics Technol. Lett.* **8**, 299 (1996); L. Rahman, G. Li, and F. Tian, *Opt. Commun.* **138**, 91 (1997); A. Hohl, A. Gavrielides, T. Erneux, and V. Kovanis, *Phys. Rev. Lett.* **78**, 4745 (1997).
- [18] D. N. Klimenko, N. V. Kravtsov, E. G. Lariontsev, and V. V. Firsiv, *Kvant. Elektron. (Moscow)* **24**, 649 (1997) [*Quantum Electron.* **27**, 631 (1997)].
- [19] J. R. Terry, K. S. Thornburg, Jr., D. J. DeShazer, G. D. VanWageningen, S. Zhu, P. Ashwin, and R. Roy, *Phys. Rev. E* **59**, 4036 (1999).
- [20] M. Möller, B. Forsmann, and W. Lange, *Quantum Semiclassical Opt.* **10**, 839 (1998); A. Uchida, M. Shinozuka, T. Ogawa, and K. Kannari, *Opt. Lett.* **24**, 890 (1999).
- [21] A. Barsella, C. Lepers, D. Dangoisse, P. Glorieux, and T. Erneux, *Opt. Commun.* **165**, 251 (1999).
- [22] L. Luo, P. L. Chu, T. Whitbread, and R. F. Peng, *Opt. Commun.* **175**, 213 (2000).
- [23] K. Otsuka, R. Kawai, S-L. Hwong, J-Y. Ko, and J-L. Chern, *Phys. Rev. Lett.* **84**, 3049 (2000).
- [24] R. H. Measures, *Laser Remote Sensing: Fundamentals and Application* (Wiley, New York, 1984).
- [25] E. P. Velikhov, V. Yu. Baranov, V. S. Letokhov, E. A. Ryabov, and A. N. Starostin, *Pulsed CO₂ Lasers and Their Application for Isotope Separation* (Nauka, Moscow, 1983).
- [26] I. M. Bertel', V. O. Petukhov, S. A. Trushin, and V. V. Churakov, *Pis'ma Zh. Tekh. Fiz.* **6**, 1501 (1980) [*Sov. Tech. Phys. Lett.* **6**, 647 (1980)]; D. M. Tratt, A. K. Kar, and R. G. Harrison, *J. Phys. E* **15**, 1010 (1980).
- [27] V. A. Gorobets, K. V. Kozlov, B. F. Kuntsevich, and V. O. Petukhov, *Kvant. Elektron. (Moscow)* **27**, 21 (1999) [*Quantum Electron.* **29**, 294 (1999)].
- [28] F. T. Arecchi, in *Instabilities and Chaos in Quantum Optics*, edited by F. T. Arecchi and R. G. Harrison (Springer-Verlag, Berlin, 1987).
- [29] B. F. Kuntsevich, A. N. Pisarchik, and V. V. Churakov, *Infrared Phys. Technol.* **40**, 313 (1999).
- [30] A. N. Pisarchik, B. F. Kuntsevich, and R. Corbalán, *Phys. Rev. E* **57**, 4046 (1998); B. F. Kuntsevich and A. N. Pisarchik, *J. Opt. B: Quantum Semiclassical Opt.* **1**, 349 (1999).
- [31] K. Smith and R. M. Tomson, *Computer Modeling of Gas Lasers* (Plenum Press, New York, 1978).
- [32] B. F. Gordiets, A. I. Osipov, and L. A. Shelepin, *Kinetic Processes in Gases and Molecular Lasers* (Nauka, Moscow, 1980).
- [33] V. V. Churakov, V. A. Gorobets, and V. O. Petukhov, *Infrared Phys.* **29**, 339 (1989).
- [34] M. I. Rabinovich and D. I. Trubetskov, *Introduction to Theory of Oscillations and Waves* (Nauka, Moscow, 1984).
- [35] D. V. Ramana Reddy, A. Sen, and G. L. Johnston, *Physica D* **129**, 15 (1999).
- [36] S. A. Zenchenko, S. V. Leshkevich, A. I. Portniagin, S. P. Puchek, and A. E. Filipov, *Kvant. Elektron. (Moscow)* **17**, 841 (1990) [*Sov. J. Quantum Electron.* **20**, 760 (1990)].
- [37] C. O. Weiss and R. Vilaseca, *Dynamics of Lasers* (VCH, Weihaim, 1991).
- [38] A. A. Andronov, A. A. Witt, and S. E. Khaikin, *Theory of Oscillations* (Nauka, Moscow, 1981).
- [39] A. S. Biryukov, N. I. Lipatov, P. P. Pashinin, and A. M. Prokhorov, *Kvant. Elektron. (Moscow)* **16**, 195 (1989) [*Sov. J. Quantum Electron.* **19**, 127 (1989)].